# Seismic SSI Analysis of ISFSI on Sloping Rock Foundation Using $^{MTR/}$SASSI

Mansour Tabatabaie[1], Basilio Sumodobila[1], Paul Baughman[2], Bobby Marlar[3] and Luie Starnes[3]

1) SC Solutions, Inc., Walnut Creek, CA, U.S.A.
2) ARES Corporation, Stratham, NH, U.S.A.
3) Duke Energy ONS, Seneca, SC, U.S.A.

**ABSTRACT**

The Independent Spent Fuel Storage Installation (ISFSI) at the Oconee nuclear power station needs to be expanded in order to accommodate the continued on-site storage of spent fuel. A proposed Phase VI expansion will extend the existing reinforced concrete basemat approximately 130 feet to the south. In addition, a future Phase VII expansion will be located immediately south of the proposed Phase VI expansion. A geotechnical investigation of the proposed Phase VI and VII expansions finds that the foundation basemats will be founded on soil material over sloping rock. The thickness of the soil layer roughly increases from zero feet near the northern edge of the Phase VI basemat to about 50 feet beyond the southern edge of the Phase VII basemat. To further quantify the subsurface soil and rock material characteristics and to analyze their effects on the ISFSI basemat design, a soil-structure interaction (SSI) analysis was performed using the $^{MTR/}$**SASSI** program.

This paper describes the process of 3-D SSI analysis incorporating sloping rock conditions below the foundation basemat in $^{MTR/}$**SASSI**. The procedure has been validated against available solutions, and the results of the seismic response of the ISFSI facility, using this methodology, are presented for various loading configurations of Horizontal Storage Modules (HSMs).

## INTRODUCTION

The existing on-site ISFSI at the Oconee nuclear power station consists of five phases (I, II, III, IV and V). The proposed ISFSI Phase VI expansion will extend the existing reinforced concrete basemat at Phase V approximately 130 feet to the south, and will support 24 Transnuclear Model 102 Horizontal Storage Modules (HSMs). In addition, a future Phase VII expansion will be located immediately south of Phase VI. Figure 1 shows a pictorial view of existing ISFSI Phases I-V as well as future expansion Phases VI-VII. Figure 2 shows a plan view of the ISFSI basemats for Phases I-VII. A geotechnical investigation of the proposed Phase VI and VII expansions finds that the foundation basemats will be founded on soil material over sloping rock. The thickness of the soil layer roughly increases from zero feet near the northern edge of the proposed Phase VI basemat to about 50 feet beyond the southern edge of the Phase VII basemat. To further quantify the subsurface soil and rock material characteristics and to analyze their effects on the ISFSI basemat design, a soil-structure interaction (SSI) analysis was performed using the $^{MTR/}$**SASSI** program.

In the SSI analysis a numerical finite element (FE) model of the ISFSI structures and foundations was developed using structural and soil/rock properties. The soil/rock model incorporated sloping rock characteristics at the ISFSI site and included uncertainties in the material properties by analyzing best estimate (BE), upper range (UR) and lower range (LR) soil/rock cases. In addition, the SSI analysis considered the coupling effects of the existing and new ISFSI phases. A single set of three-component acceleration time histories were used as input, and a total of eleven (11) load cases corresponding to different configurations of the ISFSI basemats and their HSM loadings were analyzed:

- Load Case A: Fully loaded basemats for existing Phases I-V
- Load Cases B1-B5: Fully loaded basemats for existing Phases I-V plus fully and/or partially loaded basemats for Phase VI
- Load Cases C1-C5: Fully loaded basemats for existing Phases I-VI and fully and/or partially loaded basemats for Phase VII

Dead load and live load analyses were also performed, and the results were combined with seismic demand.

The following sections consist of a description of the methodology employed to analyze seismic SSI response of the ISFSI founded on sloping rock foundation using $^{MTR/}$**SASSI**, details of the model development and analysis cases, and a summary of selected analysis results and discussions.


**Figure 1 – Pictorial View of ISFSI Phases I-VII**

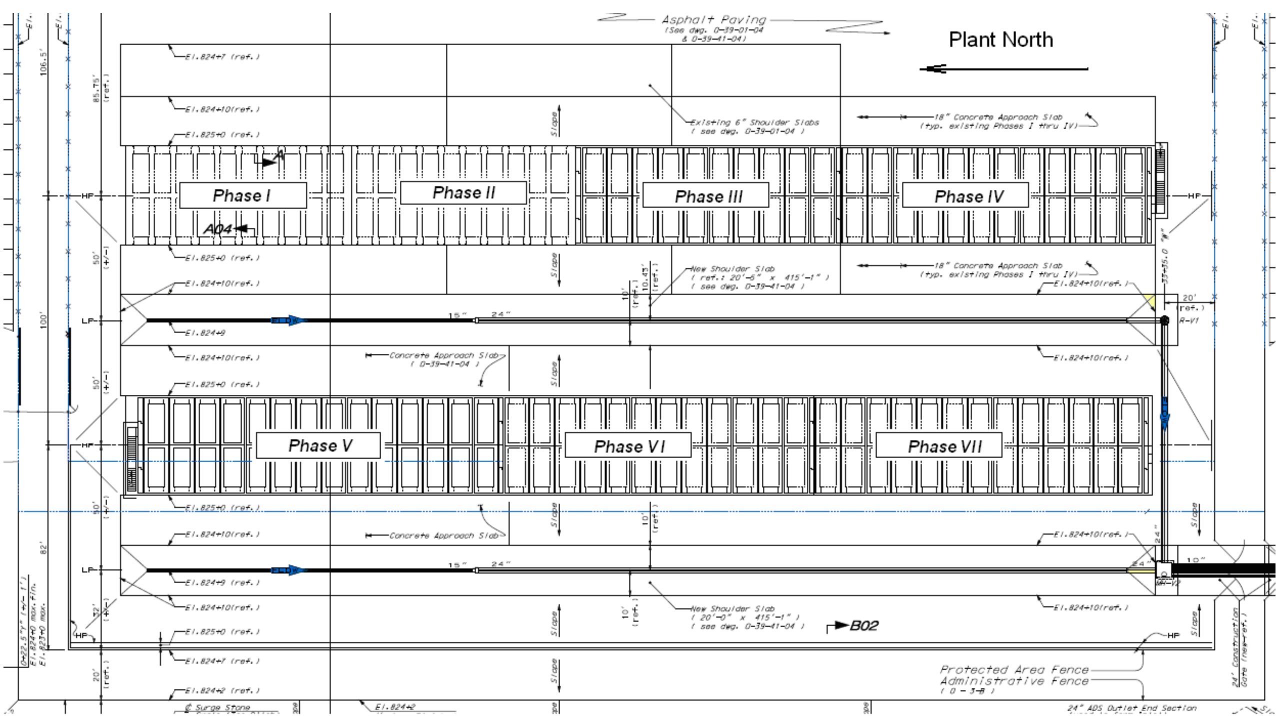


**Figure 2 – Plan View of ISFSI Basemats for Phases I-VII**

## METHODOLOGY

Seismic SSI analysis consisted of the following analyses:

### Site Response Analysis

One-dimensional soil column analysis was performed by the computer program SHAKE91 [1] to determine strain-compatible soil properties for site response and SSI analyses. SHAKE91 computes the response of a semi-infinite horizontally layered soil deposit overlying a uniform half-space subjected to vertically propagating shear waves. Analysis is performed in the frequency domain; therefore, for any set of properties analysis is linear. Nonlinear soil behaviors are accounted for through an iterative procedure. The object motion (i.e., motion that is known) can be specified at the top of any sublayer within the soil profile or at the corresponding outcrop.

Site response analysis was performed using the computer program $^{MTR/}$**SASSI** [2] to develop scattered motions for SSI analysis. $^{MTR/}$**SASSI** uses finite element and complex frequency response methods to calculate the dynamic response of structures supported in a horizontally layered soil system over uniform half-space. The primary soil material nonlinearities in $^{MTR/}$**SASSI** are the strain-compatible soil shear modulus and damping ratios calculated from the 1-D soil column analysis. For site response (wave scattering) analysis, a new feature in $^{MTR/}$**SASSI** was utilized which allows sloping rock conditions below the structure to be incorporated.

### SSI Analysis

SASSI [3] treats the far-field soils as a horizontally layered system over uniform halfspace. In 3-D models, incorporating sloping rock conditions below the structure foundation dramatically increases the size of the model to be analyzed. It then becomes almost impossible to analyze through the conventional SASSI approach. An efficient method to solve the 3-D SSI problem for sloping rock condition has been developed and incorporated into $^{MTR/}$**SASSI**. The procedure consists of solving the scattering problem from a 2-D plane-strain $^{MTR/}$**SASSI** model subject to the incidence of in-plane SV- and P-waves and out-of-plane SH-waves, and incorporating the results as input motion to a 3-D SSI model with "sloping rock interaction node" option. Figure 3 shows the $^{MTR/}$**SASSI** sub-structuring scheme for the sloping rock model analysis. The analysis procedure consists of the following steps:

Step 1: Develop a 2-D plane-strain free-field scattering soil model with sloping rock condition using $^{MTR/}$**SASSI**.

Step 2: Analyze the 2-D scattering model for in-plane and out-of-plane response to develop three components of input motion corresponding to the interaction nodes of a 3-D SSI model.

Step 3: Develop a 3-D SSI model incorporating a grid of interaction nodes on the sloping rock surface.

Step 4: Analyze the 3-D SSI model using the scattered motions obtained from Step 1.

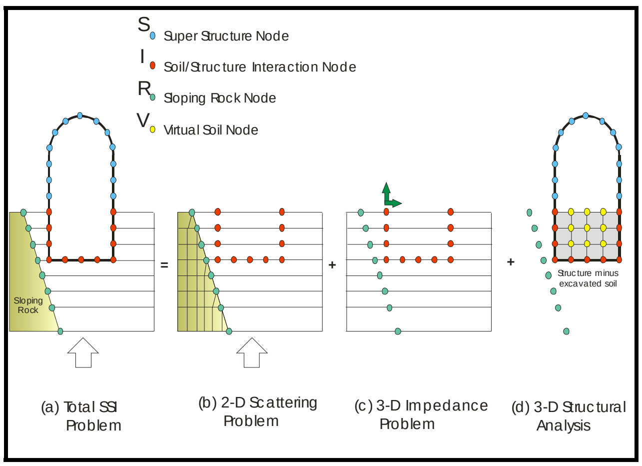


**Figure 3 - $^{MTR/}$SASSI Sub-Structuring Model for Sloping Rock Condition**

## INPUT GROUND MOTIONS

The input motion specified for the site response and SSI analyses is the El Centro, N/S Component acceleration time history recorded during the 1940 Imperial Valley earthquake. This motion is linearly scaled to a 0.1g maximum acceleration and used as outcropping rock motion at the ISFSI site for both horizontal and vertical components. The acceleration time history of the 1940 El Centro, N/S Component and its acceleration response spectra for 5% damping is shown in Figure 4.

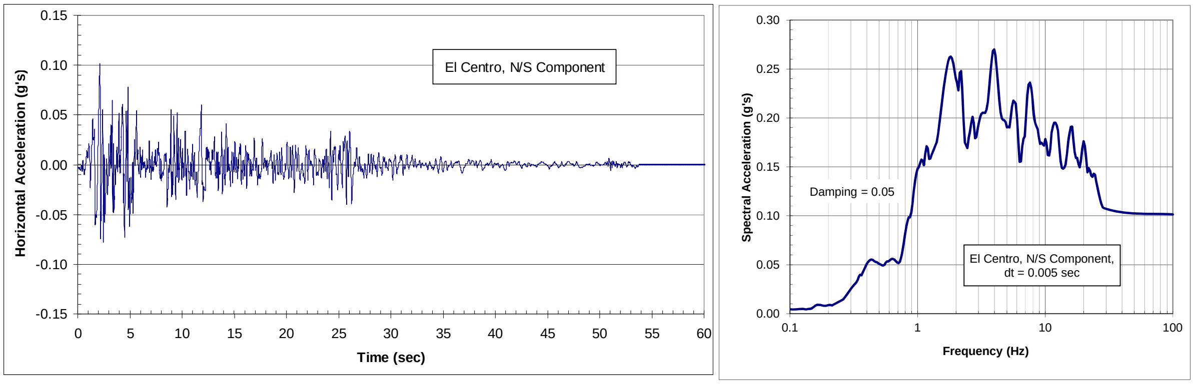


**Figure 4 - Acceleration Time History and Response Spectra of Input Outcrop Rock Motion**

## SOIL AND ROCK PROFILE AND PROPERTIES

Based on available geotechnical information, an idealized soil profile of the ISFSI site was developed for site response and SSI analyses. This profile, which shows the variation of soil and rock conditions along the long axis of the ISFSI basemats (approx. N-S direction), is shown in Figure 5. In the direction transverse to the ISFSI basemats (approx. E-W direction) the profile is uniform. The primary site response issue is seismic wave scattering due to sloping rock conditions in the N-S direction along the long axis. This condition is characterized by a plane-strain soil model in the N-S direction (see Figure 5). The idealized profile shows the soil/rock layering and configurations in relation to the ISFSI basemats, which are underlain by varying thicknesses of soil overlying the rock formation. Three sets of soil and rock properties representing lower range (LR), upper range (UR) and best estimate (BE) soil properties were used for site response and SSI analyses. The small-strain dynamic soil layer properties are shown in Table 1.

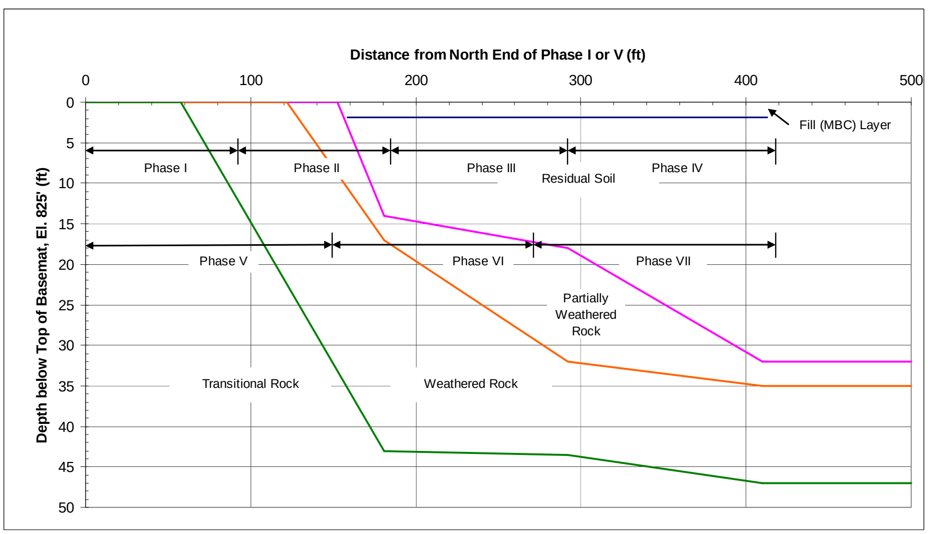


**Figure 5 - Idealized Soil Profile in N-S Direction**

**Table 1 - Dynamic Soil Properties**

| Layer Name | Moist Unit Weight (pcf) | Saturated Unit Weight (3) (pcf) | $V_s$ Best Estimate (2) (ft/sec) | Poisson's Ratio, $\upsilon$ | Shear Modulus, $G$ (ksf) | Young's Modulus, $E$ (ksf) | $V_s$ Lower Range (ft/sec) | $V_s$ Upper Range (ft/sec) |
|---|---|---|---|---|---|---|---|---|
| Fill (MBC) | 142 | 147 | 1456 | 0.30 (1) | 9349 | 24,307 | 971 | 2184 |
| Residual Soil | 111 | 122 | 702 | 0.49 | 1699 | 5062 | 468 | 1053 |
| Partially Weathered Rock | 142 | 142 | 1435 | 0.48 (4) | 9081 | 26,880 | 957 | 2152 |
| Weathered Rock | 160 | 160 | 2588 | 0.46 | 33,281 | 97,180 | 1725 | 3882 |
| Transitional Rock | 170 | 170 | 4302 | 0.36 | 97,709 | 265,768 | 2868 | 6453 |

## SITE RESPONSE ANALYSIS

One-dimensional shear-wave propagation analysis of the far-field soil column was performed for the LR, UR and BE soil cases using SHAKE91 to calculate strain-compatible soil shear modulus and damping ratios for use in site response and SSI models. Input motion was assigned as outcropping motion at the surface of the transition rock. Free-field ground surface motions calculated from the 1-D site response analysis were later compared to far-field motions calculated from seismic wave scattering analysis. In addition to horizontal motion, the vertical soil column response was calculated for the LR, UR and BE soil cases subject to vertically propagating P-waves. The 5% damped horizontal and vertical acceleration response spectra at the ground surface for the LR, UR and BE soil column cases are shown in Figure 6.

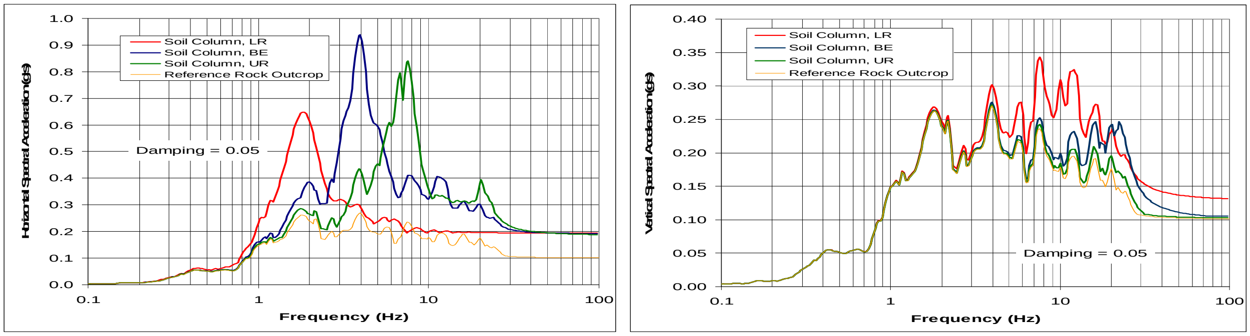


**Figure 6 – Free-Field Ground Surface Response Spectra - 1-D Site Response Analysis**

To account for the effects of seismic wave scattering due to sloping rock conditions at the ISFSI site, two-dimensional, plane-strain site response analysis was performed using MTR/**SASSI**. Two finite element (FE) models were developed. Model 1 consists of a plane-strain FE mesh with two in-plane translational degrees-of-freedom (DOFs) per node to simulate P-, SV- and R-wave propagations. Model 2 consists of a similar plane-strain FE model with one out-of-plane translational DOF per node to model SH- and L-wave propagations. The 3-D configuration and layout of the ISFSI interaction nodes and sloping rock boundary nodes are shown in Figures 7(a) and 7(b), respectively.

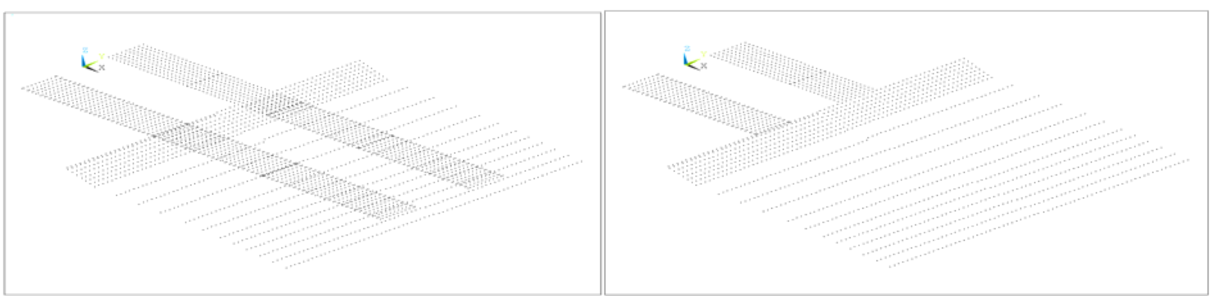

(a) Interaction Nodes (b) Sloping Rock Boundary Nodes

**Figure 7 - 3-D MTR/SASSI Interaction and Sloping Rock Boundary Nodes**

The soil portion of the 2-D site response FE model was extended 500 feet southward from the southern edge of the Phase IV (or VII) basemat to minimize the impact of wave reflections at the lateral soil boundaries. Figure 8 shows a schematic view of the site response models. The in-plane model was subjected separately to vertically propagating P- and SV-waves with respective vertical and horizontal control motions specified at the base rock. The out-of-plane model was subjected to vertically propagating SH-waves with horizontal control motion also specified at the base rock. Three models corresponding to the LR, UR and BE soil cases were analyzed. The iterated soil and rock properties obtained from the corresponding 1-D soil column analysis were used in the site response model. Figure 9 shows the 2 D FE model used to calculate the site response.

To verify that no reflections occur at the base and/or lateral boundaries, ground motions computed at the far left (rock) top corners of the site response models were compared with input rock outcrop. The same type of comparison was made for ground motions calculated at the far right (soil) top corners of the models against soil column responses calculated by both MTR/SASSI 2-D and SHAKE91 1-D. The results showed that the site response models correctly predicted the far-field rock and soil motions, thus validating their accuracy in calculating ground response at ISFSI locations underlain by sloping rock conditions.

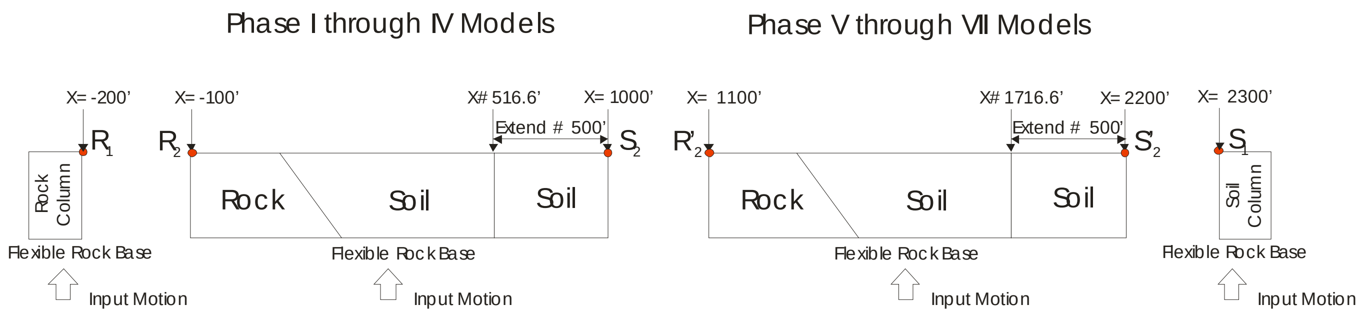


**Figure 8 - Schematic View of Scattering Models**

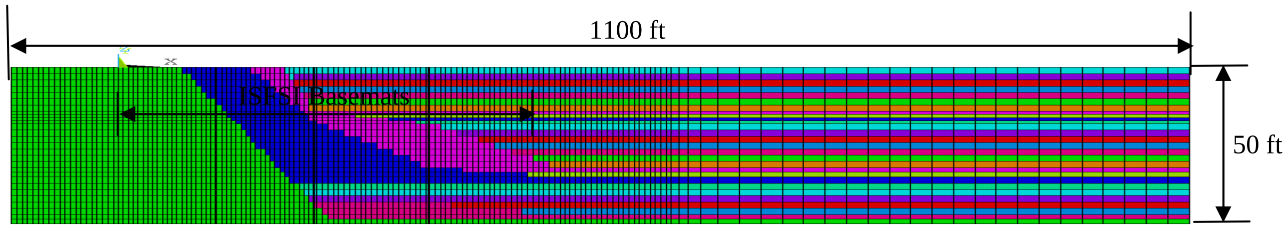


**Figure 9 - 2-D Plane-Strain FE Model Used for Site Response Analysis**

**SSI ANALYSIS**

The ISFSI basemats were modeled using 3-D plate/shell elements incorporating in-plane membrane action and out-of-plane flexural behavior with un-cracked concrete properties. The ISFSI basemats for the HSM modules at the Oconee Nuclear Station consist of reinforced concrete slabs. For Phases I-II, the HSMs are cast in place with concrete basemats. These HSMs were modeled with a lumped mass attached to a rigid frame connected to the basemat with rigid springs, as shown in Figure 10(a). The HSMs' frequencies occupy the rigid range due to their box-like configuration. For Phases III-VII, the HSMs consist of pre-fabricated modules with Dry Storage Canisters (DSCs). They are modeled with a single lumped mass, located at the center of gravity (c.g.) of the HSM, connected to a beam element. The beam element for each HSM/DSC is connected at the bottom to a rigid perimeter frame that is, in turn, connected to the basemat by rigid vertical springs at the corners and by rigid horizontal springs at the middle of the perimeter beams. This connection scheme avoids any artificial stiffening of the basemat at the HSM footprints since storage modules for Phases III-VII simply rest on the top of the basemat. Figure 10(b) shows details of the HSM/DSC model for Phases III-VII.

Structural properties of the HSMs, DSCs, and basemats were provided by the manufacturer. The stiffness of vertical beams for the Phases III-VII HSMs/DSCs were calibrated such that horizontal and vertical modes equal $f_x$=17 Hz, $f_y$=33 Hz and $f_z$=40 Hz. For dead load analysis, HSMs were modeled to provide uniform distribution of HSM loading onto slabs.

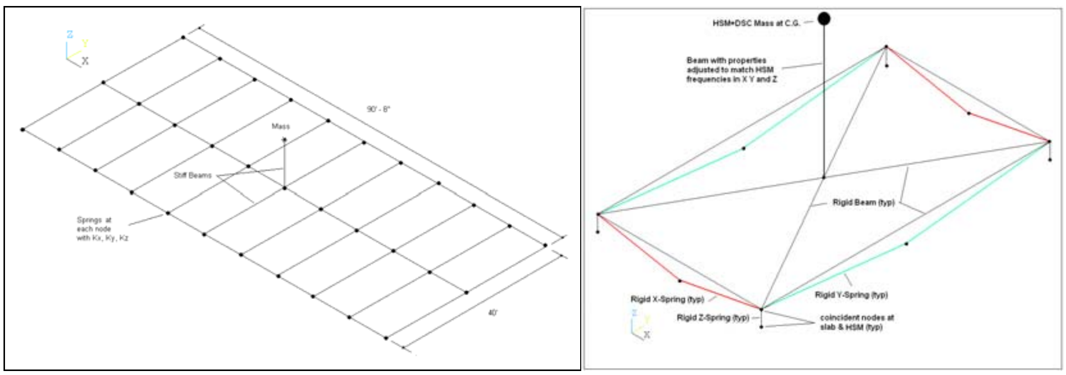

(a) Phases I-II

(b) Phases III-VII

**Figure 10 - Finite Element Model of HSM/DSC**

Three-dimensional MTR/**SASSI** FE models of the ISFSI facility were developed for seismic SSI analysis using the basemat and HSM properties described above. Corresponding SSI models were also developed for dead load analysis. The analysis cases are described below.

Model A: This model incorporates fully loaded basemats for existing Phases I-V (Load Case A).

Model B: This model incorporates fully loaded basemats for existing Phases I-V plus proposed Phase VI. A total of 5 DSC load cases (B1-B5) for Phase VI were considered. For these loading configurations, the fully loaded Phase VI basemat and its HSMs were assumed to be in place.

Model C: This model incorporates fully loaded basemats for existing Phases I-V plus fully loaded basemats for Phase VI and future Phase VII. A total of 5 DSC load cases (C1-C5) for Phase VII were considered. Again, for these loading configurations the fully loaded Phase VII basemat and its HSMs were assumed to be in place.

The SSI FE model for Models B and C are shown in Figure 11.

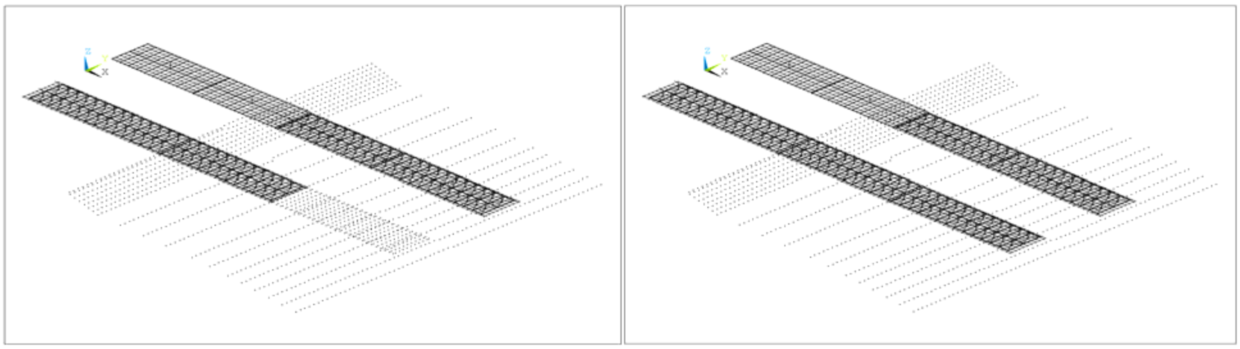

(a) Phases I-VI Basemats (b) Phases I-VII Basemats

**Figure 11 - 3-D MTR/SASSI SSI Model of ISFSI**

## ANALYSIS RESULTS

A total of 99 seismic SSI analyses (11 load cases x 3 soil cases x 3 input motions) were performed. Input motions were applied in the global x-, y- and z-directions, corresponding to the long axis of basemats (N-S), short axis of basemats (E-W) and vertical direction, respectively. The input motions consisted of the scattered motions calculated above. In addition to seismic analyses, dead load and live load analyses were also performed. A total of 33 dead plus live load cases (11 structural load cases x 3 soil cases) were analyzed. Dead load analyses included the weight of basemat and end walls. Live load analyses included the weight of HSMs and DSCs. No additional live loads were applied since the basemat is fully occupied by HSMs. The analyses provide the static stresses and forces of the basemats.

Maximum accelerations at the c.g. of the HSMs/DSCs were computed for each of the basemats for all load cases (A, B1-B5 and C1-C5) and soil cases (LR, UR and BE). The co-directional maximum accelerations calculated from input in the x-, y-, and z-directions were combined using the Square Root of the Sum of the Squares (SRSS) rule. The maximum acceleration responses enveloped for all three soil cases for Load Cases A, B1-B5 and C1-C5 are shown in Table 2.

**Table 2 – Maximum Acceleration Responses Enveloped for All Soil Cases**

| Slab | Load Case A | | | Load Cases B1-B5 | | | Load Cases C1-C5 | | |
|---|---|---|---|---|---|---|---|---|---|
| | X-Acc. | Y-Acc. | Z-Acc. | X-Acc. | Y-Acc. | Z-Acc. | X-Acc. | Y-Acc. | Z-Acc. |
| Phase I | 0.103 | 0.103 | 0.102 | 0.103 | 0.103 | 0.102 | 0.103 | 0.103 | 0.102 |
| Phase II | 0.118 | 0.132 | 0.108 | 0.118 | 0.132 | 0.108 | 0.118 | 0.132 | 0.108 |
| Phase III | 0.228 | 0.248 | 0.136 | 0.289 | 0.261 | 0.144 | 0.237 | 0.255 | 0.143 |
| Phase IV | 0.280 | 0.276 | 0.143 | 0.289 | 0.284 | 0.144 | 0.302 | 0.296 | 0.144 |
| Phase V | 0.180 | 0.214 | 0.149 | 0.167 | 0.151 | 0.114 | 0.167 | 0.151 | 0.114 |
| Phase VI | | | | 0.238 | 0.256 | 0.162 | 0.229 | 0.247 | 0.143 |
| Phase VII | | | | | | | 0.217 | 0.201 | 0.143 |

Maximum forces and moments in each of the basemats were calculated for Load Cases A, B1-B5 and C1-C5 and soil cases LR, UR and BE. The results included the SRSS of maximum forces and moments per unit length of slab from the input accelerations applied in the x-, y- and z-directions, SRSS (EQ), dead load plus live load (DL + LL) and load combination (EQ + 1.0 DL + 1.0 LL).

Typical results of maximum forces and moments computed in each of the basemats and enveloped for all soil cases for Load Cases B5 and C5 are summarized in Tables 3 and 4, respectively. To evaluate the adequacy of the basemats, the P-M capacity was calculated based on cross-sectional and strength properties. The slab is 36 inches thick, reinforced with No. 11 bars spaced 12 inches apart from top to bottom of the slab. In calculating the P-M capacity, compressive strength of the concrete is 5,000 psi and rebar yield stress is 60,000 psi. Typical results for all basemats together with calculated P-M demand for Load Cases B5 and C5 are shown Figures 12(a) and 12(b), respectively. Tensile force combined with the bending moment causes critical stresses in the concrete and rebar, and governs the P-M demand versus capacity evaluation.

**Table 3 - Computed Maximum Forces and Moments Enveloped for All Soil Cases, Load Case B5**

| Slab | Load Combination 1.0(DL+LL) + 1.0EQ | | | | | | |
|---|---|---|---|---|---|---|---|
| | N1 (k/ft) | N2 (k/ft) | N12 (k/ft) | M1 (k-ft/ft) | M2 (k-ft/ft) | S1 (k/ft) | S2 (k/ft) |
| Phase I | 4.629 | 0.787 | 2.365 | 0.189 | 0.035 | 0.067 | 0.009 |
| Phase II | 35.548 | 12.459 | 19.457 | 26.490 | 14.056 | 15.785 | 3.546 |
| Phase III | 99.631 | 37.442 | 27.723 | 76.530 | 83.594 | 32.943 | 38.863 |
| Phase IV | 81.286 | 27.866 | 18.720 | 76.683 | 86.188 | 26.682 | 28.573 |
| Phase V | 49.068 | 8.328 | 18.471 | 1.264 | 0.209 | 1.204 | 0.084 |
| Phase VI | 66.499 | 28.211 | 16.673 | 62.407 | 80.822 | 22.477 | 37.027 |
| Phase VII | | | | | | | |

**Table 4 - Computed Maximum Forces and Moments Enveloped for All Soil Cases, Load Case C5**

| Slab | Load Combination 1.0(DL+LL) + 1.0EQ | | | | | | |
|---|---|---|---|---|---|---|---|
| | N1 (k/ft) | N2 (k/ft) | N12 (k/ft) | M1 (k-ft/ft) | M2 (k-ft/ft) | S1 (k/ft) | S2 (k/ft) |
| Phase I | 4.629 | 0.787 | 2.365 | 0.189 | 0.035 | 0.067 | 0.009 |
| Phase II | 36.220 | 13.051 | 20.068 | 26.657 | 13.509 | 15.857 | 3.504 |
| Phase III | 106.197 | 38.481 | 28.009 | 77.425 | 84.373 | 33.394 | 39.133 |
| Phase IV | 83.817 | 29.294 | 19.518 | 76.985 | 86.882 | 26.652 | 29.024 |
| Phase V | 49.085 | 8.332 | 18.471 | 1.263 | 0.209 | 1.204 | 0.083 |
| Phase VI | 105.318 | 33.909 | 20.970 | 60.278 | 82.177 | 25.090 | 37.331 |
| Phase VII | 86.456 | 30.436 | 19.760 | 79.172 | 86.881 | 26.505 | 28.897 |

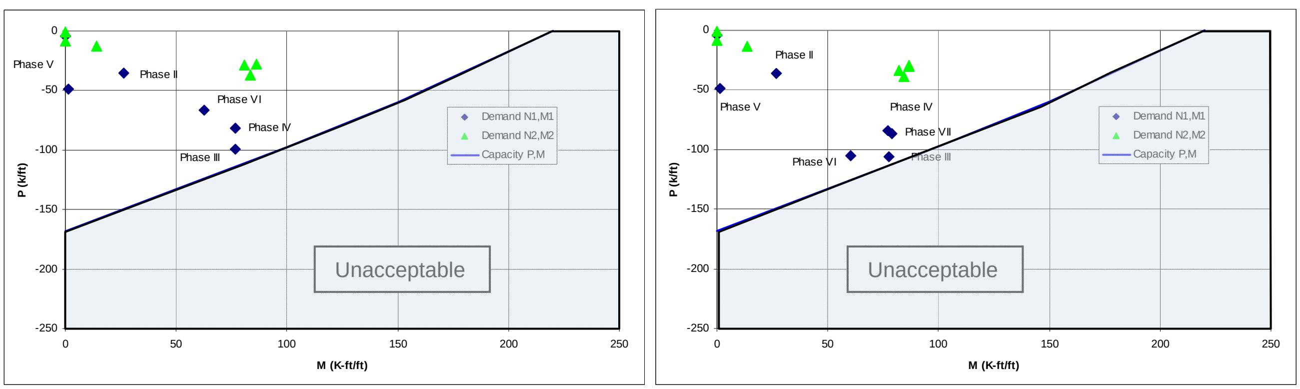


(a) Load Case B5

(b) Load Case C5

**Figure 12 - P-M Demand vs. Capacity Enveloped for All Soil Cases**

## REFERENCES

1. SHAKE91 (1992), "A Computer Program for Conducting Equivalent Linear Seismic Response Analyses of Horizontally Layered Soil Deposits," Department of Civil & Environmental Engineering, University of California, Davis.

2. MTR/**SASSI** (2008), "System for Analysis of Soil-Structure Interaction," Version 7.04, MTR & Associates, Inc., Lafayette, California.

3. Lysmer, J., Tabatabaie, M., Tajirian, F., Vahdani, S. and Ostadan, F. (1981), "SASSI – A System for Analysis of Soil-Structure Interaction," Report No. UCB/GT/81-02, Geotechnical Engineering, Department of Civil Engineering, University of California, Berkeley.